



The Dysregulation and Prognostic Analysis of STRIPAK Complex Across Cancers

Ruiling Xie*, Feng Wen and Yong Qin*

Department of Otolaryngology, Head and Neck Surgery, Peking University First Hospital, Beijing, China

OPEN ACCESS

Edited by:

Cesare Indiveri,
University of Calabria, Italy

Reviewed by:

Ulrich Kück,
Ruhr University Bochum, Germany
Hao Zhou,

Chinese People's Liberation Army
General Hospital, China
Anna Schmidt,
Western Colorado University,
United States

*Correspondence:

Ruiling Xie
rxl@bjmu.edu.cn
Yong Qin
youngcaptain@sina.com

Specialty section:

This article was submitted to
Cellular Biochemistry,
a section of the journal
Frontiers in Cell and Developmental
Biology

Received: 22 January 2020

Accepted: 23 June 2020

Published: 10 July 2020

Citation:

Xie R, Wen F and Qin Y (2020)
The Dysregulation and Prognostic
Analysis of STRIPAK Complex Across
Cancers. *Front. Cell Dev. Biol.* 8:625.
doi: 10.3389/fcell.2020.00625

The striatin-interacting phosphatase and kinase (STRIPAK) is the highly conserved complex, which gains increased attention in physiology and pathology process recently. However, limited studies reported the details of STRIPAK complex in cancers while some results strongly suggested it plays a vital role in tumorigenesis. Hence, we systematically analyzed the molecular and survival profiles of 18 STRIPAK genes to assess the value of STRIPAK complex across cancers. Our findings revealed the low frequencies of DNA aberrances and incomparable expression difference of STRIPAK genes between normal and tumor tissues, but they showed strong prognostic value in cancers, especially the liver hepatocellular carcinoma (LIHC) and kidney renal clear cell carcinoma (KIRC). Interestingly, STRIPAK genes were observed the opposite pattern of survival and expression in the above two cancer types. PPP2R1A and TRAF3IP3 were proposed as the oncogenic genes in LIHC and KIRC, respectively. The STRIPAK genes serve as oncogenes may due to the methylation heterogeneity. Taken together, our comprehensive molecular analysis of STRIPAK complex provides resource to facilitate the understanding of mechanism and utilize the potential therapies to tumors.

Keywords: STRIPAK, bioinformatical analysis, cancer, prognosis, PPP2R1A, TRAF3IP3

INTRODUCTION

The striatin-interacting phosphatase and kinase (STRIPAK) is a conserved complex during the evolution, which consists of the scaffolding subunit PPP2R1A (also known as PP2AA), catalytic subunit PPP2CA (also known as PP2AC), and regulatory subunit striatins (STRNs) containing STRN, STRN3, and STRN4 (Goudreault et al., 2009; Frost et al., 2012) (**Figure 1A** and **Supplementary Table S1**). Striatins recruit striatin-interacting protein 1/2 (STRIP1/2, also known as FAM40A/B), MOB4, PDCD10 (also known as CCM3). PDCD10 interacts with and stabilizes germinal center kinase III (GCK III) family, which consists of three genes, STK24 (also known as MST3), STK25 (also known as YSK1), and STK26 (also known as MST4) (Fidalgo et al., 2010). The investigators predicted that two heteromeric models of the STRIPAK complex, the difference are the binding proteins to STRIP1/2. The interaction to CTTNBP2 family is the complex I, and complex II contains sarcolemmal membrane-associated protein (SLMAP), TRAF3IP3, SIKE1 and FGR1OP2 (Goudreault et al., 2009). The dynamic assembly of STRIPAK complexes regulates the downstream effectors (Chen et al., 2018; Chen R. et al., 2019; Tang et al., 2019).

The importance of STRIPAK is highlighted in physiological processes (Hwang and Pallas, 2014; Kuck et al., 2019), such as apoptosis (Chen et al., 2009), Golgi assembly (Fidalgo et al., 2010; Kean et al., 2011), and embryo, vascular and neural development (He et al., 2010; Sakuma et al., 2014, 2016; Ultanir et al., 2014; Bazzi et al., 2017; Gil-Ranedo et al., 2019). For example, deletion or mutation of *strip1* in mouse embryos caused distinguishable mesoderm morphogenesis (Bazzi et al., 2017), while knockdown of *strip* in *Drosophila* showed disturbance in early endosome organization (Sakuma et al., 2014). Another regulators in STRIPAK complex, STK24 promotes development of spine synapse via thousand and-one amino acid kinases TAOK1 and TAOK2 associated with Myosin Va axis (Ultanir et al., 2014). The conserved STRIPAK complex regulates the reactivation of *Drosophila* neural stem cells through functioning as a switch to Hippo pathway and InR/PI3K/Akt signaling (Gil-Ranedo et al., 2019). Moreover, STRIPAK plays an important role in human diseases, including heart failure, diabetes, autism, and cerebral cavernous malformation (CCM) (Hwang and Pallas, 2014). For instance, PDCD10 mutations are responsible for CCM (Guclu et al., 2005; Chen et al., 2009), and loss of PDCD10 dissociated ZO-1 and actin via phosphorylation of cortactin, which caused instability of tight junction complex and consequently impairment of brain barrier integrity (Stamatovic et al., 2015). Furthermore, STRIPAK serves as the node of active signaling that contributes to broad implications. The cellular localization of STRIPAK components indicated STRIPAK bridge organelles, such as the nuclear membrane, the centrosome, and Golgi (Guzzo et al., 2004; Fidalgo et al., 2010; Frost et al., 2012; Hwang and Pallas, 2014).

Researchers summarized that STRIPAK complexes play critical roles in cancer (Shi et al., 2016). The components of STRIPAK were identified as the regulators of actomyosin cytoskeleton (Bai et al., 2011; Madsen et al., 2015; Bazzi et al., 2017), determining their roles in the migrate mode of cancer cell via controlling the Ezrin/Radixin/Moesin family proteins (Madsen et al., 2015). Besides the migrate ability, different groups reported that the STRIPAK complex regulates the Hippo pathway in various processes (Ribeiro et al., 2010; Sakuma et al., 2016; Bae et al., 2017; Gil-Ranedo et al., 2019; Tang et al., 2019), including tumor progression (Yu et al., 2015; Chen et al., 2018; Kim et al., 2020). MST1/2 and MAP4Ks, which belong to STE20 kinase family, interact with STRIPAK via core components in *Drosophila* and mammalian cells (Goudreault et al., 2009; Tang et al., 2019). In our previous study, we verified the binding via co-immunoprecipitation assay and founded that STRIPAK initiates the Hippo pathway via RhoA/RHPN1 activation upon upstream signals (Chen R. et al., 2019). Recently, both findings of Madsen lab and our lab showed that STRIPAK complexes controlled oncogenic transformation via regulation of MST1/2 or MAP4K4 (Chen R. et al., 2019; Rodriguez-Cupello et al., 2020).

Since the STRIPAK complex received increased attention in regulation among the signaling network and function in cancers, we provided the analysis of molecular dysregulation and clinical correlation of the STRIPAK complex across cancers using online databases. The results revealed that even though most genes encoding STRIPAK complex did not frequently harbor mutations

or copy number alterations across cancers, patients with altered genes showed unfavorable survival. Opposite survival pattern of STRIPAK genes were observed in liver hepatocellular carcinoma and kidney renal clear cell carcinoma. Our study illustrated the role of the STRIPAK complex in cancer, and the discoveries should give the insights of the STRIPAK-related molecular mechanisms and involvement in cancer.

MATERIALS AND METHODS

Gene Set Curation and PPI Network

The genes of STRIPAK complex were curated from the studies using the affinity purification and mass spectrometry approaches (Goudreault et al., 2009). The core STRIPAK genes include PPP2R1A, PPP2CA, STRIP1/2, STRN3/4, SLMAP, GCKIII family, PDCD10, MOB4, CTTNBP2/NL, FGFR1OP2, TRAF3IP3, and SIKE1. The GCKIII family contains three genes, STK24, STK25, and STK26 (**Supplementary Table S1**). Protein-protein interaction (PPI) information is evaluated by online Search Tool for the Retrieval of Interacting Genes (STRING version 11.0¹) (Szklarczyk et al., 2015). Date of the query was 2020-06-03. The organism was “*Homo sapiens*,” minimum required interaction score was 0.400 (medium confidence) and without clustering. The results of network statistics were from the “Analysis.” The visualization and analysis of PPI network is performed by Cytoscape (version 3.8.0).

GO and KEGG Enrichment Analyses of STRIPAK Genes

The Database for Annotation, Visualization and Integrated Discovery (DAVID²) (Dennis et al., 2003) (version 6.8) was applied for the functional and pathway enrichment of proteins encoded by STRIPAK genes. Gene Ontology (GO) analysis is a common bioinformatics tool for large-scale analysis of functional enrichment. The classifications of gene functions contain biological process (BP), molecular function (MF), and cellular component (CC). GO annotations of STRIPAK genes were performed using a DAVID online tool. KEGG (Kyoto Encyclopedia of Genes and Genomes) is a database resource, which provides large-scale information in molecular level and facilitates scientists to manipulate high-level functions and biological processes (Kanehisa and Goto, 2000). KEGG pathway analysis of STRIPAK genes was performed using the KOBAS online analysis database³ (Xie et al., 2011) (version 3.0), and date of the query was 2019-11-02. *p*-value of <0.05 was considered statistically significant.

Somatic Copy-Number Alteration (SCNA) and Somatic Mutation Analysis

The SCNA and somatic mutation of STRIPAK genes were analyzed and depicted using cBioPortal⁴ (Gao et al., 2013). All

¹<https://string-db.org/>

²<http://david.ncifcrf.gov>

³<http://kobas.cbi.pku.edu.cn/>

⁴<http://www.cbioportal.org/>

of analysis was performed on 18 STRIPAK genes in the set of 32 non-redundant TCGA PanCancer Atlas studies containing 10967 samples. The date of the query was 2020-06-10.

Prognostic Power of STRIPAK Genes

The overall survival (OS) and disease-free survival (DFS) of STRIPAK genes were analyzed by cBioPortal (Gao et al., 2013), GEPIA2⁵ (Tang et al., 2017), Kaplan–Meier plotter⁶, UALCAN⁷ (Chandrashekar et al., 2017), LOGpc⁸ (Xie et al., 2019) and MethSurv⁹ (Modhukur et al., 2018) which are the online tools for visualization, evaluation and download of large-scale cancer-related genomics data sets. The Kaplan–Meier curves in cBioPortal were applied to evaluate the prognostic power of STRIPAK genes with genetic alterations in patients harboring cancer. The survival map was generated by GEPIA2 to screen the prognostic value of STRIPAK genes in cancers, which we selected “0.05” as the significance level, and “Median” as the group cutoff. The survival map of GSE29609 and GSE76427 was generated by R packages pheatmap. The prognostic value of STRIPAK genes in 371 samples of liver cancer and 530 samples of kidney renal clear cell carcinoma (KIRC) were performed using from the Kaplan–Meier plotter mRNA (RNAseq) pan-cancer database. The expression level of each gene was grouped by best cutoff and months of survival were selected as survival time units. *p*-value of < 0.05 was considered statistically significant. The combined survival analysis of TCGA and GEO database were performed using the online consensus survival for LIHC (OSlihc) and KIRC (OSkirc) of LOGpc, which data source was “combined” and split patients by “Upper 50%” or “Upper 25%.” The survival analysis of DNA methylation was performed using MethSurv, which split by “best” option to dichotomize methylation profiles without adjust for co-variables.

Expression of STRIPAK Genes in Human Samples and Cancer Cell Lines

The expression profiles of STRIPAK genes in normal and tumor tissues between LIHC and KIRC were analyzed and/or showed using OncoPrint¹⁰ (Rhodes et al., 2004), GEPIA2, UALCAN, the Cancer Proteome Atlas (TCPA¹¹) (Li et al., 2013) and R packages pheatmap. We used the following parameters of Multiple Genes Comparison in GEPIA2: “Yes” for Log Scale, and “Matched TCGA normal data.” To identify the differentially expression proteins between LIHC and KIRC, we took advantages of the function named “Differential Analysis” under “Individual Cancer Analysis” in TCPA. OncoPrint is an online cancer microarray database that provides a platform to discover genome-wide expression differences. We screened tumor studies in OncoPrint database with include criteria as follows: (a) Cancer Type: LIHC or KIRC, (b) “Gene: PPP2R1A,”

⁵<http://gepia2.cancer-pku.cn/>

⁶<http://kmplot.com/analysis/>

⁷<http://ualcan.path.uab.edu/>

⁸<http://bioinfo.henu.edu.cn/DatabaseList.jsp>

⁹<https://biit.cs.ut.ee/methsurv/>

¹⁰<http://www.oncoPrint.com/>

¹¹<https://tcpaportal.org/tcpa/index.html>

(c) “Analysis Type: Cancer vs. Normal Analysis” and (d) Threshold setting condition (*p* < 0.05, Fold change > 1.5, gene rank = all). The correlation between the clinical-pathological parameters and expression level or methylation profiles of STRIPAK were analyzed using UALCAN. The co-expression of TRAF3IP3 and Src family tyrosine kinase (LCK) were analyzed using cBioportal and TCPA. The DNA methylation profiles of TRAF3IP3 in KIRC were performed using the function named “Gene visualization” in MethSurv.

The comparison of STRIPAK genes between liver cancer cell lines and kidney cancer cell lines was performed based on the data extracted from the Cancer Cell Line Encyclopedia (CCLE¹²) (Barretina et al., 2012). We extracted RNAseq data of liver and kidney cancer cell lines from CCLE with the criteria as follows, (a) matched cancer type; (b) none problematic or contaminated; (c) had values. The annotations of cell lines were performed according to the ExPasy Cellosaurus¹³. Finally, 21 kinds of liver cancer cell lines and 12 kinds of kidney cancer cell lines were included in our study.

Statistical Analysis

The statistical tests were performed using R software (version 3.6.1). We used *t*-test (two-tailed) or *Mann-Whitney* test for comparison between two groups. We used the *Schoenfeld* individual test to evaluate the proportional hazards assumption for the fit of Cox regression model. The survival analysis of survival was performed using univariate and multivariate Cox proportional hazards model, which split by optimal cutoff values, which were generated by the “surv_cutpoint” function of R package survminer (Kassambara et al., 2019), to dichotomize expression level. A value of *p* < 0.05 was considered statistically significant, **p* < 0.05, ***p* < 0.01, ****p* < 0.001.

RESULTS

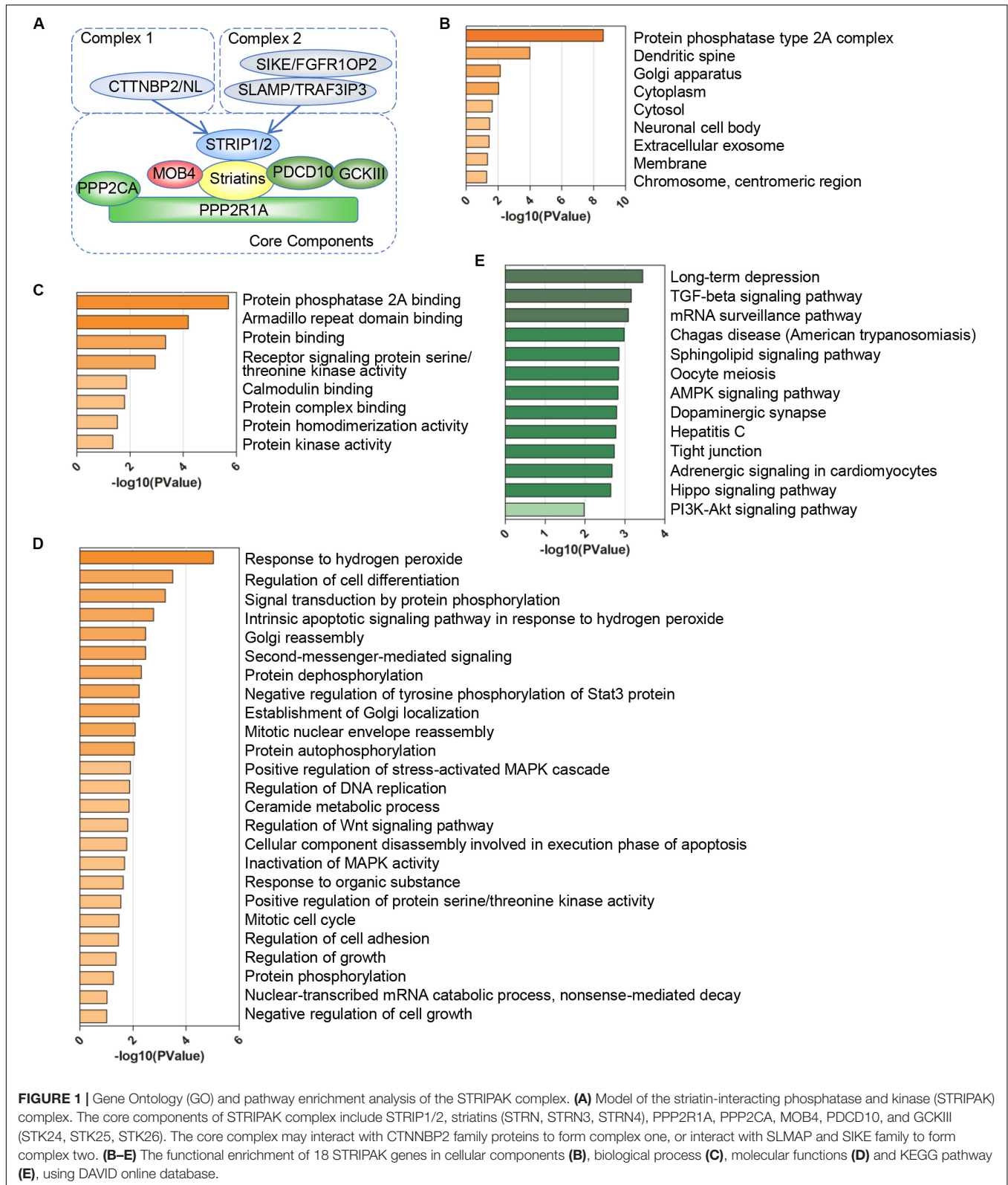
Gene Oncology and Pathway Enrichment of STRIPAK

To verify our data set (Figure 1A), we constructed the PPI network of STRIPAK complex via STRING online tool. The average local clustering coefficient of the PPI network is 0.992 and *p*-value of PPI enrichment is less than 1.0e-16, which suggests that the connections of STRIPAK proteins are dense. To understand deeply among STRIPAK complex, we performed GO functions and KEGG pathway enrichment analysis using online tools of DAVID and KOBAS. There was no surprise that the enrichment showed that STRIPAK relates to the protein phosphatase type 2A complex and regulates the signal transduction by phosphorylation and dephosphorylation (Figures 1B–D).

Gene ontology enrichment analysis showed that genes encoded STRIPAK were enriched in cellular components, including dendritic spine and Golgi apparatus (Figure 1B);

¹²<https://portals.broadinstitute.org/ccle/>

¹³<https://web.expasy.org/cellosaurus/>



biological processes, including armadillo repeat domain binding and receptor signaling protein serine/threonine kinase activity (**Figure 1C**); and molecular functions,

including response to hydrogen peroxide and regulation of cell differentiation (**Figure 1D**). KEGG pathway analysis showed that STRIPAK genes were significantly enriched in long-term

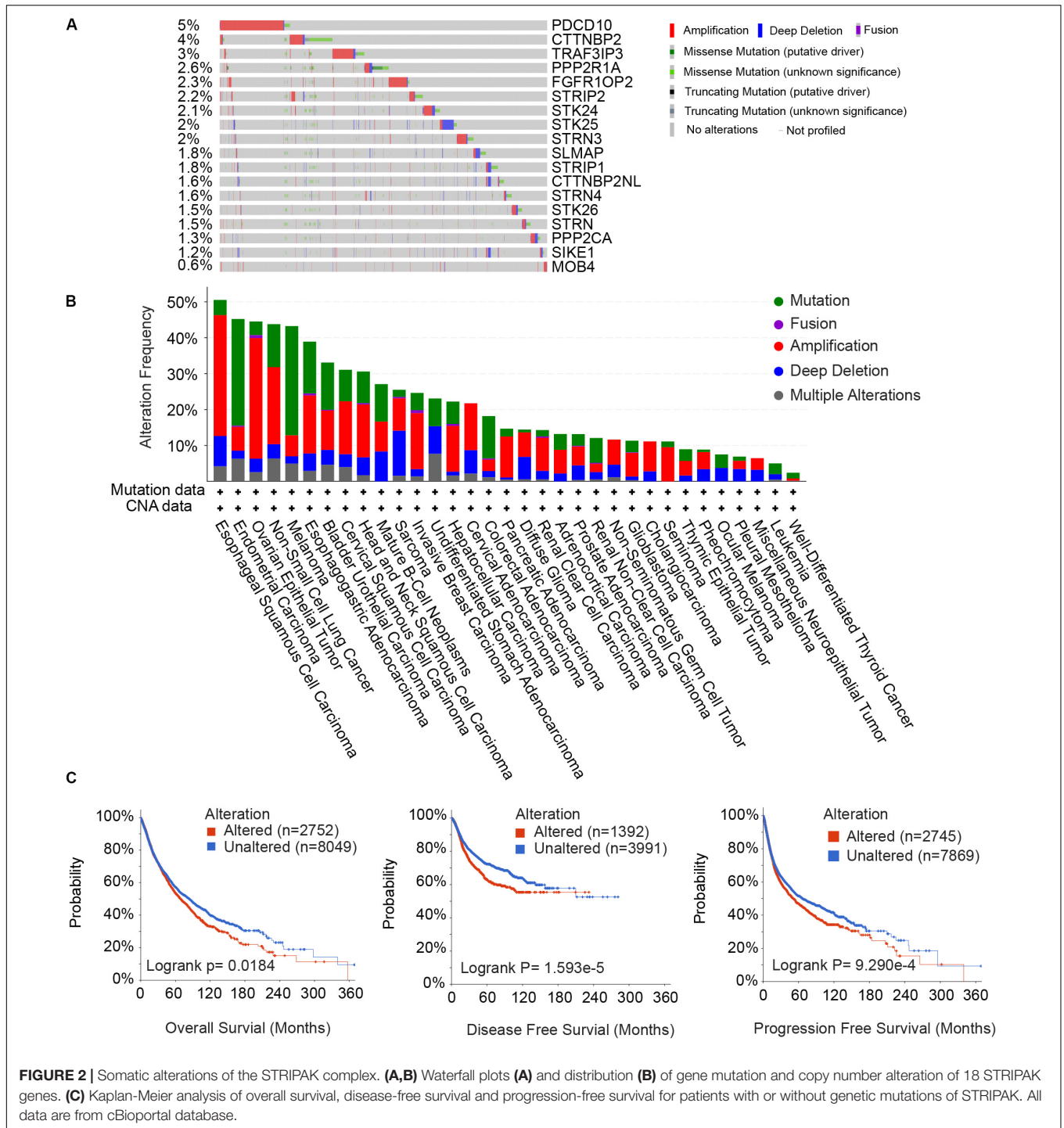


FIGURE 2 | Somatic alterations of the STRIPAK complex. **(A,B)** Waterfall plots **(A)** and distribution **(B)** of gene mutation and copy number alteration of 18 STRIPAK genes. **(C)** Kaplan-Meier analysis of overall survival, disease-free survival and progression-free survival for patients with or without genetic mutations of STRIPAK. All data are from cBioportal database.

depression, TGF-beta signaling pathway and mRNA surveillance pathway (Figure 1E).

Molecular Alteration Landscape of the STRIPAK Complex

Since the STRIPAK complex is important for physiological and pathological processes, we focused on the genetic

alterations of STRIPAK genes across cancers. We calculated the somatic copy number alteration (SCNA) and mutation frequency in pan-cancer cohort of 10967 patients using cBioportal (Figures 2A,B). The overall DNA aberration was low, ranging from 0.6 to 5%. PDCD10 ranked the highest altered frequency, followed by CTTNBP2, TRAF3IP3, and PPP2R1A. Amplification was the predominant type of STRIPAK aberration. Surprisingly, altered STRIPAK genes

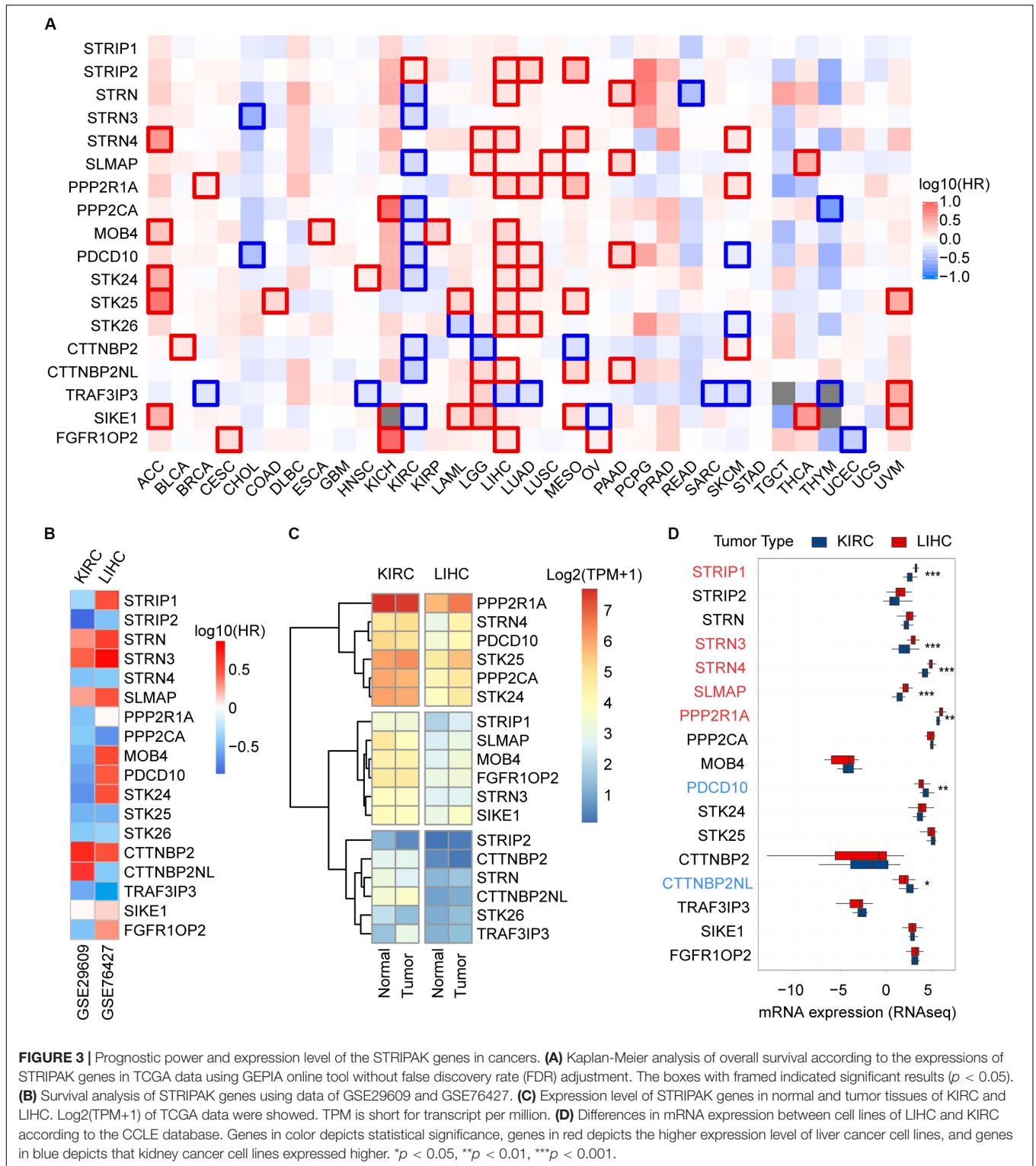
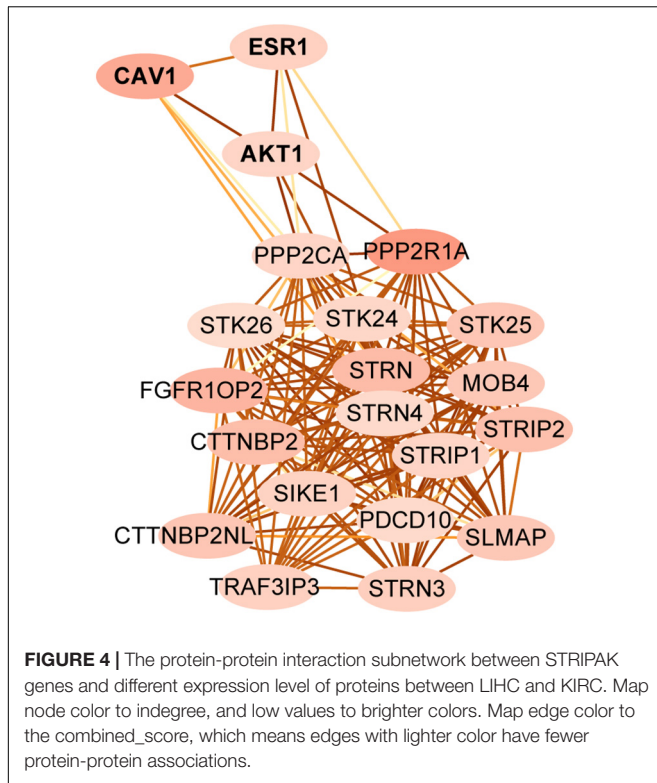


FIGURE 3 | Prognostic power and expression level of the STRIPAK genes in cancers. **(A)** Kaplan-Meier analysis of overall survival according to the expressions of STRIPAK genes in TCGA data using GEPIA online tool without false discovery rate (FDR) adjustment. The boxes with framed indicated significant results ($p < 0.05$). **(B)** Survival analysis of STRIPAK genes using data of GSE29609 and GSE76427. **(C)** Expression level of STRIPAK genes in normal and tumor tissues of KIRC and LIHC. Log₂(TPM+1) of TCGA data were showed. TPM is short for transcript per million. **(D)** Differences in mRNA expression between cell lines of LIHC and KIRC according to the CCLE database. Genes in color depicts statistical significance, genes in red depicts the higher expression level of liver cancer cell lines, and genes in blue depicts that kidney cancer cell lines expressed higher. * $p < 0.05$, ** $p < 0.01$, *** $p < 0.001$.

are present in 50.53% (48/95 cases) of patients with esophageal squamous cell carcinoma and 38.91% (200/514 cases) of patients with esophagogastric adenocarcinoma (Figure 2B). Thus, STRIPAK genes with DNA aberration might be involved in esophageal carcinoma. The aberration of STRIPAK genes

showed the unfavorable overall survival (OS), disease-free survival (DFS) and progression-free survival (Figure 2C), which suggested the significance of STRIPAK dysregulation across cancers on the account for the landscape of somatic alteration and mutation.



Prognostic Power and Differential Expression of STRIPAK Genes Across Cancers

To unravel prognostic value of STRIPAK genes across cancer types, we screened the correlation of their expression with patients' survival using GEPIA2 and Kaplan–Meier plotter. The abbreviations of cancer type were summarized in **Supplementary Table S2**. The results of survival analysis showed that many STRIPAK genes had significant survival across cancer (**Figure 3A** and **Supplementary Figures S1–S3**). Liver hepatocellular carcinoma (LIHC) had 16 significant genes, which ranked the highest cancer type, followed by kidney renal clear cell carcinoma (KIRC) that had 15 significant genes (**Supplementary Table S3** and **Supplementary Figures S2, S3**). Even though only 14.48% (151/1043) cases harbored the genetic alterations, LIHC patients

with DNA aberration showed unfavorable overall survival and disease-free survival (**Supplementary Figure S2D**).

Surprisingly, opposite patterns were observed in the above top 2 cancer types with or without false discovery rate (FDR) adjustment of p -value (**Figure 3A** and **Supplementary Figures S1–S3**). Opposite to LIHC patients, KIRC patients with high expressions of STRIPAK genes showed favorable survival (**Figure 3A** and **Supplementary Figure S3**). To confirm the survival prediction patterns of STRIPAK between KIRC and LIHC, we analyzed GSE29609 and GSE76427 by splitting the group by optimum value of gene expression level. The result was consistent with survival map generated by GEPIA2 (**Figure 3B** and **Supplementary Figures S2C, S3C**). To conclude, the high expression level of whole STRIPAK complex might serve as the tumor suppressor in KIRC, while serve as oncogenic role in LIHC.

To confirm whether this pattern was due to the expression difference exists in two cancer types, we compared the mRNA expression level with the normal and tumor tissues using the same database. The results showed that STRIPAK expressed higher in KIRC tissues than in LIHC tissues, but seldom genes were found as significant difference between normal and tumor tissues in each cancer type (**Figures 3C, 5A, 6A**). The differentially expression was also detected between cancer cell lines between KIRC and LIHC (**Figure 3D**). Thus, these results indicated that STRIPAK complex might relate to prognosis of patients with cancer, and play opposite roles between KIRC and LIHC.

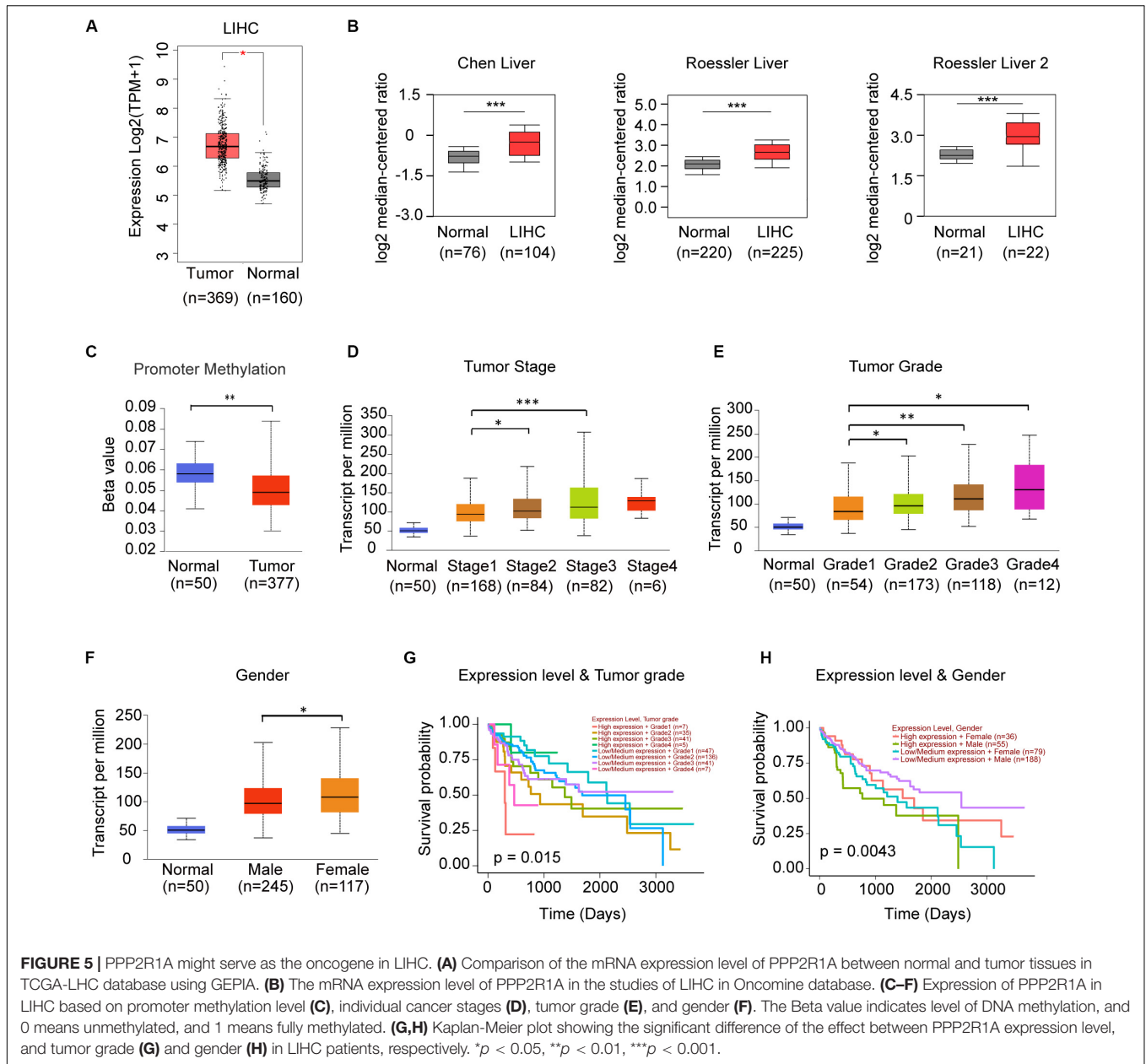
Identify Potential Targets to Explore the Role of STRIPAK Complex Between KIRC and LIHC

Striatin-interacting phosphatase and kinase is a multifunctional complex, which is regulated by many upstream signals and regulates many downstream pathways (Hwang and Pallas, 2014). To identify targets that associate with STRIPAK in KIRC and LIHC, we first compared the expressed proteins between two cancer types using TCPA. Two hundred and seventeen entries were reported as the differentially expressed protein. Since the total protein and phosphorylated protein were encoded as same gene, we submitted 174 genes of 217 entries and 18 STRIPAK genes to STRING for analyzing the PPI network. (Data not shown.) Then, we selected PPP2R1A as the central node to

TABLE 1 | Different expression levels of selected protein between KIRC and LIHC using TCPA.

Protein_Marker_ID	Gene	RPPA protein abundances*		p -value
		KIRC	LIHC	
AKT	AKT1,AKT2,AKT3	-0.71841	-0.042755	5.25E-58
AKT_pT308	AKT1,AKT2,AKT3	-0.36531	0.24294	2.59E-38
AKT_pS473	AKT1,AKT2,AKT3	-0.02963	0.51806	5.31E-19
CAVEOLIN1	CAV1	-0.28233	1.215	5.81E-80
ERALPHA	ESR1	-0.72737	-1.6739	5.13E-63
ERALPHA_pS118	ESR1	-0.32523	-0.44399	2.56E-09

*RPPA: Reverse phase protein array

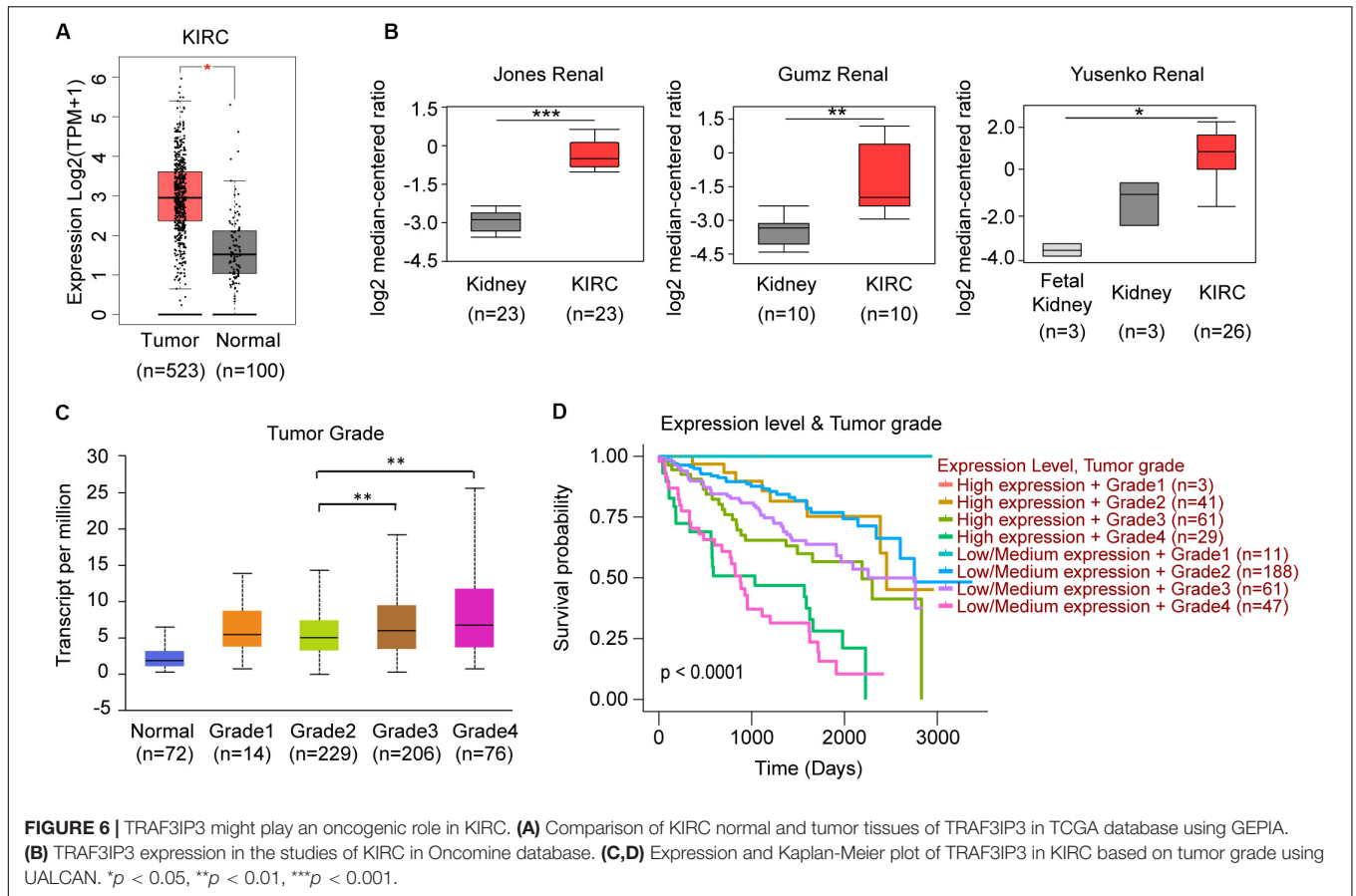


create subnetwork (Figure 4) because of the value of indegree. The connections of STRIPAK components were dense according to the subnetwork. AKT serine/threonine kinase 1 (AKT1), caveolin1 (CAV1) and estrogen receptor 1 (ESR1) were in the subnetwork, and the expression level of above proteins expressed higher in LIHC than KIRC (Table 1). The results indicated that AKT1, CAV1 and ESR1 could be the targets to explore the function of STRIPAK between KIRC and LIHC.

PPP2R1A Might Serve as the Oncogene in LIHC

Since frequency of DNA alteration was low in each genes of STRIPAK complex in LIHC (Data not shown), we speculated that

gene expression might be responsible for the prognostic power. We compared the expression level of STRIPAK genes between normal tissue and tumor tissue via GEPIA2, discovered that only PPP2R1A were observed significant difference (Figure 5A). In Oncomine database, we identified 3 of 8 studies that showed significant increased expression in tumor tissue, including Chen liver (GSE3500) and Roessler liver (GSE14520) (Figure 5B). The promoter methylation level of PPP2R1A was not parallel to the expression level, lower methylation were observed in LIHC tumor tissues while the expression level is higher (Figures 5A,C). Expression of PPP2R1A significantly correlated with tumor stage, tumor grade as well as gender (Figures 5D–F). Then, we evaluated the prognostic role of expression level of PPP2R1A and clinical parameters in LIHC. The results showed that PPP2R1A



expression level accompanied with tumor grade or gender significantly correlated with overall survival (Figures 5G,H). Taken together, PPP2R1A might serve as an oncogene in LIHC.

TRAF3IP3 Might Play an Oncogenic Role in KIRC

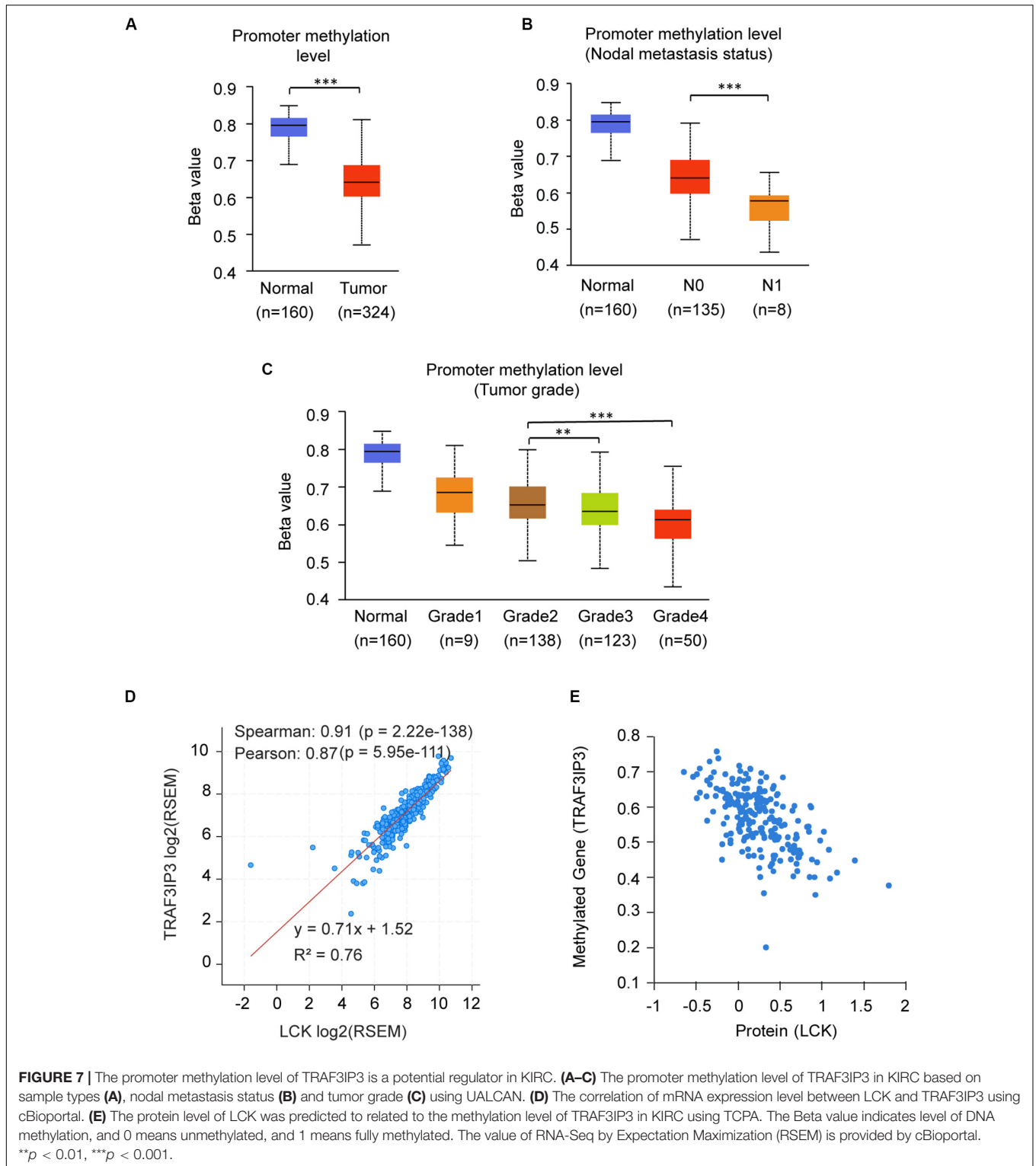
When we compared the expression between normal kidney and KIRC tissues, only TRAF3IP3 showed significant difference (Figure 6A). In the analysis of 6 studies containing KIRC in Oncomine database, 3 showed significant increased expression of TRAF3IP3. (Figure 6B) The 3 studies were Jones Renal (GSE15641), Gumz Renal (GSE6344), and Yusenko Renal (GSE11151). Except tumor grade (Figure 6C), the correlation between the expression of TRAF3IP3 and clinicopathological features showed no significance performed by UALCAN (Data not show). KIRC patients with low or medium expression of TRAF3IP3 and low tumor grade possibly had a good overall survival (Figure 6D).

The promoter methylation of TRAF3IP3 was observed higher in normal tissue than KIRC tissue (Figure 7A), and related with tumor grade and nodal metastasis status (Figures 7B,C). The results suggested that DNA methylation of TRAF3IP3 involved in the tumorigenesis of KIRC. To better know the driver genes of TRAF3IP3, we searched the TCGA database and found the protein level of Src family tyrosine kinase (LCK) negatively

correlated with the methylated TRAF3IP3 ($R = -0.57479$, $p < 0.05$), while LCK positively correlated with TRAF3IP3 in mRNA expression level (Figures 7D,E). Then, we identified single CpG sites (cg05959508, cg08655071, cg19099296, and cg10382148) as potential functional sites of TRAF3IP3 through MethSurv because of the significant prognostic value (Figure 8). Taken together, the methylation of TRAF3IP3 might be a candidate to play a role in tumorigenesis of KIRC.

DISCUSSION

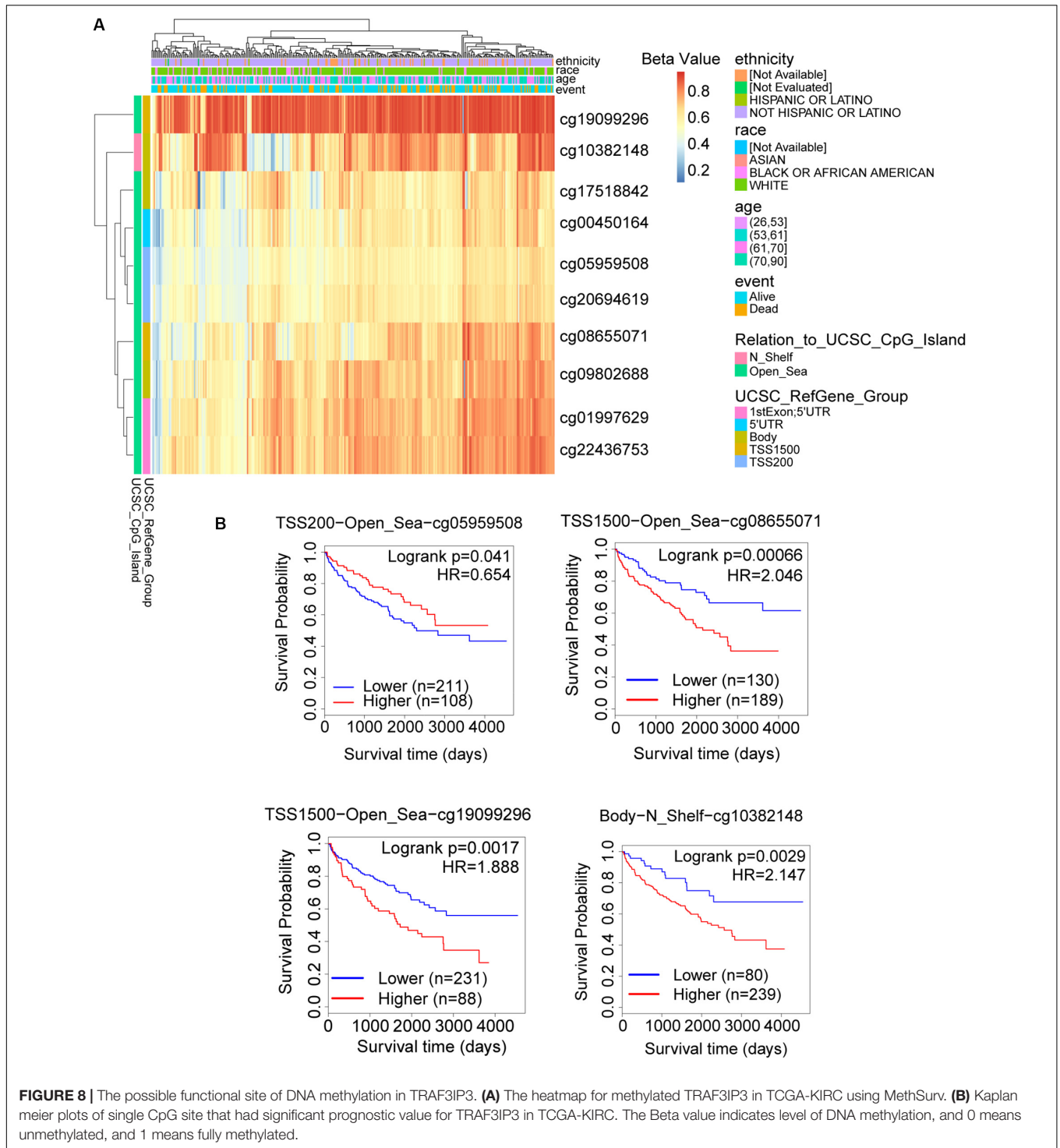
Cancer ranks as top of the leading causes of death around world in the 21st century, and the rapidly increasing incidence and mortality of cancer urge people to reduce burden through prevention and intervention against tumor (Bray et al., 2018). As the emerging star in biological process, limited articles reported STRIPAK complex play a role in tumorigenesis recently. Thus we performed molecular profiles of STRIPAK complex across cancer using online tools to analyze multi-dimensional characterization of clinical data. Unlike previous researches (Madsen et al., 2015; Chen et al., 2018; Chen R. et al., 2019), which focused on few cancer types, our results revealed that the DNA aberrations, expression and methylation, and prognostic power of STRIPAK complex across over 20 cancer types. Furthermore, PPP2R1A and TRAF3IP3 were identified as the



novel potential oncogenic genes through the integrated analysis in liver hepatocellular carcinoma (LIHC) and kidney renal clear cell carcinoma (KIRC), respectively.

One significant contribution of this study is that we illustrated dysregulated STRIPAK complex drove diverse mechanisms to

involve in the tumor progression. First is the mutation-driven mechanism. Our analysis revealed that poor survivals were showed in patients harboring altered STRIPAK genes and high-frequency aberrations were observed in specific cancer types, such as esophageal carcinoma. The individual mutated STRIPAK



gene expressed tumor-related phenotype (Madsen et al., 2015; Kim et al., 2020). Second is the protein-protein regulation. In this study, we identified AKT1, CAV1 and ESR1 as candidates to discover the function of STRIPAK complex between KIRC and LIHC. It is well established that the ATK1 is one of major substrates for protein phosphatase 2A (PP2A) (Seshacharyulu et al., 2013), which is indicated as the function of STRIPAK via the

GO enrichment analysis (Figure 1). Third is post-transcriptional regulation. In this study, few differences of expression level were found in STRIPAK genes across cancer. Hence, we turned to assess protein post-transcriptional modifications. There were significantly comparable methylation levels of PPP2R1A and TRAF3IP3 between normal and tumor tissue. Other modifications could be studied in the future to dig up the

mechanisms of STRIPAK complex. The last is dynamic complex assembly. Even though the core components of STRIPAK complex were well known, the interaction among components were still elucidated. Dynamic assembly of STRIPAK regulates the cell proliferation, migration and invasion of cancer (Chen et al., 2018; Chen R. et al., 2019; Tang et al., 2019; Rodriguez-Cupello et al., 2020). This could explain why the expression homogeneity was found between the normal and tumor samples.

DNA methylation is an impactful epigenetic modification in STRIPAK complex. Since the contrary phenotypes of PPP2R1A and TRAF3IP3 were observed in expression level and methylation level (Figures 5A,C, 6A, 7A), there is a reasonable assumption that PPP2R1A or TRAF3IP3 losses methylation may induce its stabilization. The methylation level of TRAF3IP3 gradually reduced with increased tumor grade and lymph node metastasis status (Figures 7B,C). Thus, we proposed that the methylation of STRIPAK genes might drive tumor progression via the downstream effectors as well as methylated YAP promotes tumorigenesis via increasing YAP/TEAD transcription (Fang et al., 2018). We also proposed that Src family tyrosine kinase (LCK) reversely regulated TRAF3IP3 methylation based on correlation analysis using cBioportal and TCPA (Gao et al., 2013; Chen M. M. et al., 2019) (Figures 7D,E). LCK, which belongs to Src-like non-receptor tyrosine kinase family, might lay upstream of TRAF3IP3, because knockout *Traf3ip3* in CD4⁺CD8⁺ double-positive thymocytes did not show difference in phosphorylation and expression of LCK compared with *Traf3ip3*^{+/+} cells (Zou et al., 2015). Moreover, the reversibility of DNA methylation is the promising targets for therapy (Kulis and Esteller, 2010).

There were many shortcomings in this study. First, we did not apply the experimental approaches to represent our computational results. However, the results from different groups could illustrate our discoveries. For example, our analysis uncovered that cancer patients with altered STRIPAK genes showed unfavorable survival (Figure 2C). Other group reported that the mutants of truncated STRIP2, which were found in lung adenocarcinoma and uterine carcinoma, loss the ability to bind with PPP2CA and drove cell contraction, underlying their role in cancer (Madsen et al., 2015). The MST4-MOB4 complex disassociates the assembly of MST1-MOB1 complex in pancreatic cancer, which promote cell proliferation and migration via inhibition of LATS and YAP phosphorylation (Chen et al., 2018). In addition, more information is needed to explain confused results. On the contrary of the TCGA data, 71.43% (5/7 significant genes) showed higher expression level in KIRC cell lines than LIHC cell lines, including STRIP1, STRN3, STRN4, SLMAP, and PPP2R1A (Figures 3C,D). The comparison suggested that we should be more careful for verification and implication of STRIPAK complex on cell lines based on expression-related phenotypes.

To conclude, the dysregulation of STRIPAK complex play crucial roles in different cancer contexts, especially in liver

hepatocellular carcinoma and kidney renal clear cell carcinoma. The valuable resource derived from our systematic and molecular analyses of this complex will advance mechanism comprehension in tumorigenesis and potential therapies to cancers.

DATA AVAILABILITY STATEMENT

The datasets generated for this study can be found in the TCGA (<https://cancergenome.nih.gov/>), CCLE (<https://portals.broadinstitute.org/ccle/>), Oncomine (<http://www.oncomine.com/>), and TCPA (<https://tcpaportal.org/tcpa/index.html>).

AUTHOR CONTRIBUTIONS

RX designed the experiments, analyzed data, and wrote and revised the manuscript. FW collected and analyzed data. YQ supervised the project. All authors discussed the results and commented on the manuscript.

FUNDING

RX is supported by a Ph.D. fellowship from the China Scholarship Council (CSC, 201706010323).

SUPPLEMENTARY MATERIAL

The Supplementary Material for this article can be found online at: <https://www.frontiersin.org/articles/10.3389/fcell.2020.00625/full#supplementary-material>

FIGURE S1 | Prognostic Power of the STRIPAK genes in cancers using GEPIA2. Kaplan-Meier analysis of overall survival with false discovery rate (FDR) adjustment (A) and disease-free survival with (B) or without FDR adjustment (C) according to the expressions of STRIPAK genes in TCGA data using GEPIA2 online tool. The boxes with framed were significant results ($p < 0.05$).

FIGURE S2 | Kaplan-Meier survival plots of STRIPAK genes in liver hepatocellular carcinoma (LIHC). (A,B) Kaplan-Meier plot showing the significant difference of STRIPAK genes in unfavorable (A) and favorable (B) survival of patients with LIHC. (C) The survival analysis of overall survival for LIHC patients in combined studies of TCGA and GEO databases. (D) Kaplan-Meier analysis of overall survival and disease-free survival for LIHC patients with or without genetic alterations of STRIPAK genes in 7 non-redundant studies via cBioPortal.

FIGURE S3 | Kaplan-Meier survival plots of STRIPAK genes in kidney renal clear cell carcinoma (KIRC). (A,B) Kaplan-Meier plot showing the significant difference of STRIPAK genes in unfavorable (A) and favorable (B) survival of patients with KIRC. (C) The survival analysis of overall survival for KIRC patients in combined studies of TCGA and GEO databases.

TABLE S1 | STRIPAK components in *Homo sapiens*.

TABLE S2 | The abbreviations of cancers in this study.

TABLE S3 | The prognostic information of the 18 genes of the STRIPAK complex in 21 types of cancer in Kaplan-Meier plotter.

REFERENCES

- Bae, S. J., Ni, L., Osinski, A., Tomchick, D. R., Brautigam, C. A., and Luo, X. (2017). SAV1 promotes Hippo kinase activation through antagonizing the PP2A phosphatase STRIPAK. *eLife* 6:e30278. doi: 10.7554/eLife.30278
- Bai, S. W., Herrera-Abreu, M. T., Rohn, J. L., Racine, V., Tajadura, V., Suryavanshi, N., et al. (2011). Identification and characterization of a set of conserved and new regulators of cytoskeletal organization, cell morphology and migration. *BMC Biol.* 9:54. doi: 10.1186/1741-7007-9-54
- Barretina, J., Caponigro, G., Stransky, N., Venkatesan, K., Margolin, A. A., Kim, S., et al. (2012). The cancer cell line encyclopedia enables predictive modelling of anticancer drug sensitivity. *Nature* 483, 603–607. doi: 10.1038/nature11003
- Bazzi, H., Soroka, E., Alcorn, H. L., and Anderson, K. V. (2017). STRIP1, a core component of STRIPAK complexes, is essential for normal mesoderm migration in the mouse embryo. *Proc. Natl. Acad. Sci. U.S.A.* 114, E10928–E10936. doi: 10.1073/pnas.1713535114
- Bray, F., Ferlay, J., Soerjomataram, I., Siegel, R. L., Torre, L. A., and Jemal, A. (2018). Global cancer statistics 2018: GLOBOCAN estimates of incidence and mortality worldwide for 36 cancers in 185 countries. *CA Cancer J. Clin.* 68, 394–424. doi: 10.3322/caac.21492
- Chandrashekar, D. S., Basher, B., Balasubramanya, S. A. H., Creighton, C. J., Ponce-Rodriguez, I., Chakravarthi, B., et al. (2017). UALCAN: a portal for facilitating tumor subgroup gene expression and survival analyses. *Neoplasia* 19, 649–658. doi: 10.1016/j.neo.2017.05.002
- Chen, L., Tanriover, G., Yano, H., Friedlander, R., Louvi, A., and Gunel, M. (2009). Apoptotic functions of PDCD10/CCM3, the gene mutated in cerebral cavernous malformation 3. *Stroke* 40, 1474–1481. doi: 10.1161/STROKEAHA.108.527135
- Chen, M., Zhang, H., Shi, Z., Li, Y., Zhang, X., Gao, Z., et al. (2018). The MST4-MOB4 complex disrupts the MST1-MOB1 complex in the Hippo-YAP pathway and plays a pro-oncogenic role in pancreatic cancer. *J. Biol. Chem.* 293, 14455–14469. doi: 10.1074/jbc.RA118.003279
- Chen, M. M., Li, J., Wang, Y., Akbani, R., Lu, Y., Mills, G. B., et al. (2019). TCPA v3.0: an integrative platform to explore the pan-cancer analysis of functional proteomic data. *Mol. Cell. Proteomics* 18(Suppl. 1), S15–S25.
- Chen, R., Xie, R., Meng, Z., Ma, S., and Guan, K. L. (2019). STRIPAK integrates upstream signals to initiate the Hippo kinase cascade. *Nat. Cell Biol.* 21, 1565–1577. doi: 10.1038/s41556-019-0426-y
- Dennis, G. Jr., Sherman, B. T., Hosack, D. A., Yang, J., Gao, W., Lane, H. C., et al. (2003). DAVID: database for annotation, visualization, and integrated discovery. *Genome Biol.* 4:R60.
- Fang, L., Teng, H., Wang, Y., Liao, G., Weng, L., Li, Y., et al. (2018). SET1A-mediated mono-methylation at K342 regulates YAP activation by blocking its nuclear export and promotes tumorigenesis. *Cancer Cell* 34, 103.e9–118.e9. doi: 10.1016/j.ccell.2018.06.002
- Fidalgo, M., Fraile, M., Pires, A., Force, T., Pombo, C., and Zalvide, J. (2010). CCM3/PDCD10 stabilizes GCKIII proteins to promote Golgi assembly and cell orientation. *J. Cell Sci.* 123(Pt 8), 1274–1284. doi: 10.1242/jcs.061341
- Frost, A., Elgort, M. G., Brandman, O., Ives, C., Collins, S. R., Miller-Vedam, L., et al. (2012). Functional repurposing revealed by comparing *S. pombe* and *S. cerevisiae* genetic interactions. *Cell* 149, 1339–1352.
- Gao, J., Aksoy, B. A., Dogrusoz, U., Dresdner, G., Gross, B., Sumer, S. O., et al. (2013). Integrative analysis of complex cancer genomics and clinical profiles using the cBioPortal. *Sci. Signal.* 6:11. doi: 10.1126/scisignal.2004088
- Gil-Ranedo, J., Gonzaga, E., Jaworek, K. J., Berger, C., Bossing, T., and Barros, C. S. (2019). STRIPAK members orchestrate hippo and insulin receptor signaling to promote neural stem cell reactivation. *Cell Rep.* 27, 2921.e5–2933.e5. doi: 10.1016/j.celrep.2019.05.023
- Goudreaux, M., D'Ambrosio, L. M., Kean, M. J., Mullin, M. J., Larsen, B. G., Sanchez, A., et al. (2009). A PP2A phosphatase high density interaction network identifies a novel striatin-interacting phosphatase and kinase complex linked to the cerebral cavernous malformation 3 (CCM3) protein. *Mol. Cell. Proteomics* 8, 157–171. doi: 10.1074/mcp.M800266-MCP200
- Guclu, B., Ozturk, A. K., Pricola, K. L., Bilguvar, K., Shin, D., O'Roak, B. J., et al. (2005). Mutations in apoptosis-related gene, PDCD10, cause cerebral cavernous malformation 3. *Neurosurgery* 57, 1008–1013. doi: 10.1227/01.neu.0000180811.56157.e1
- Guzzo, R. M., Sevinc, S., Salih, M., and Tuana, B. S. (2004). A novel isoform of sarcolemmal membrane-associated protein (SLMAP) is a component of the microtubule organizing centre. *J. Cell Sci.* 117(Pt 11), 2271–2281. doi: 10.1242/jcs.01079
- He, Y., Zhang, H., Yu, L., Gunel, M., Boggon, T. J., Chen, H., et al. (2010). Stabilization of VEGFR2 signaling by cerebral cavernous malformation 3 is critical for vascular development. *Sci. Signal.* 3:ra26.
- Hwang, J., and Pallas, D. C. (2014). STRIPAK complexes: structure, biological function, and involvement in human diseases. *Int. J. Biochem. Cell Biol.* 47, 118–148. doi: 10.1016/j.biocel.2013.11.021
- Kanehisa, M., and Goto, S. (2000). KEGG: kyoto encyclopedia of genes and genomes. *Nucleic Acids Res.* 28, 27–30. doi: 10.1093/nar/28.1.27
- Kassambara, A., Kosinski, M., and Biecek, P. (2019). *survminer: Drawing Survival Curves using 'ggplot2'*. Available at: <http://www.sthda.com/english/rpkgs/survminer/> (accessed May 28, 2020).
- Kean, M. J., Ceccarelli, D. F., Goudreaux, M., Sanches, M., Tate, S., Larsen, B., et al. (2011). Structure-function analysis of core STRIPAK Proteins: a signaling complex implicated in Golgi polarization. *J. Biol. Chem.* 286, 25065–25075. doi: 10.1074/jbc.M110.214486
- Kim, J. W., Berrios, C., Kim, M., Schade, A. E., Adelmant, G., Yeerna, H., et al. (2020). STRIPAK directs PP2A activity toward MAP4K4 to promote oncogenic transformation of human cells. *eLife* 9:e53003. doi: 10.7554/eLife.53003
- Kuck, U., Radchenko, D., and Teichert, I. (2019*). STRIPAK, a highly conserved signaling complex, controls multiple eukaryotic cellular and developmental processes and is linked with human diseases. *Biol. Chem.* 400, 1005–1022. doi: 10.1515/hsz-2019-0173
- Kulis, M., and Esteller, M. (2010). DNA methylation and cancer. *Adv. Genet.* 70, 27–56. doi: 10.1016/B978-0-12-380866-0.00002-2
- Li, J., Lu, Y., Akbani, R., Ju, Z., Roebuck, P. L., Liu, W., et al. (2013). TCPA: a resource for cancer functional proteomics data. *Nat. Methods* 10, 1046–1047. doi: 10.1038/nmeth.2650
- Madsen, C. D., Hooper, S., Tozluoglu, M., Bruckbauer, A., Fletcher, G., Erler, J. T., et al. (2015). STRIPAK components determine mode of cancer cell migration and metastasis. *Nat. Cell Biol.* 17, 68–80. doi: 10.1038/ncb3083
- Modhukur, V., Iljasenko, T., Metsalu, T., Lökk, K., Laisk-Podar, T., and Vilo, J. (2018). MethSurv: a web tool to perform multivariable survival analysis using DNA methylation data. *Epigenomics* 10, 277–288. doi: 10.2217/epi-2017-0118
- Rhodes, D. R., Yu, J., Shanker, K., Deshpande, N., Varambally, R., Ghosh, D., et al. (2004). ONCOMINE: a cancer microarray database and integrated data-mining platform. *Neoplasia* 6, 1–6. doi: 10.1016/s1476-5586(04)80047-2
- Ribeiro, P. S., Josue, F., Wepf, A., Wehr, M. C., Rinner, O., Kelly, G., et al. (2010). Combined functional genomic and proteomic approaches identify a PP2A complex as a negative regulator of Hippo signaling. *Mol. Cell* 39, 521–534. doi: 10.1016/j.molcel.2010.08.002
- Rodriguez-Cupello, C., Dam, M. S. L., Wang, S., Lindgren, D., Englund, E., Kjellman, P., et al. (2020). The STRIPAK complex regulates response to chemotherapy through p21 and p27. *Front. Cell Dev. Biol.* 8:146.
- Sakuma, C., Kawachi, T., Haraguchi, S., Shikanai, M., Yamaguchi, Y., Gelfand, V. I., et al. (2014). *Drosophila* Strip serves as a platform for early endosome organization during axon elongation. *Nat. Commun.* 5:5180. doi: 10.1038/ncomms6180
- Sakuma, C., Saito, Y., Umehara, T., Kamimura, K., Maeda, N., Mosca, T. J., et al. (2016). The strip-hippo pathway regulates synaptic terminal formation by modulating actin organization at the *Drosophila* neuromuscular synapses. *Cell Rep.* 16, 2289–2297. doi: 10.1016/j.celrep.2016.07.066
- Seshacharyulu, P., Pandey, P., Datta, K., and Batra, S. K. (2013). Phosphatase: PP2A structural importance, regulation and its aberrant expression in cancer. *Cancer Lett.* 335, 9–18. doi: 10.1016/j.canlet.2013.02.036
- Shi, Z., Jiao, S., and Zhou, Z. (2016). STRIPAK complexes in cell signaling and cancer. *Oncogene* 35, 4549–4557. doi: 10.1038/nc.2016.9
- Stamatovic, S. M., Sladojevic, N., Keep, R. F., and Andjelkovic, A. V. (2015). PDCD10 (CCM3) regulates brain endothelial barrier integrity in cerebral cavernous malformation type 3: role of CCM3-ERK1/2-cortactin cross-talk. *Acta Neuropathol.* 130, 731–750. doi: 10.1007/s00401-015-1479-z
- Szklarczyk, D., Franceschini, A., Wyder, S., Forslund, K., Heller, D., Huerta-Cepas, J., et al. (2015). STRING v10: protein-protein interaction networks, integrated over the tree of life. *Nucleic Acids Res.* 43, D447–D452. doi: 10.1093/nar/gku1003
- Tang, Y., Chen, M., Zhou, L., Ma, J., Li, Y., Zhang, H., et al. (2019). Architecture, substructures, and dynamic assembly of STRIPAK complexes in Hippo signaling. *Cell Discov.* 5:3. doi: 10.1038/s41421-018-0077-3

- Tang, Z., Li, C., Kang, B., Gao, G., Li, C., and Zhang, Z. (2017). GEPIA: a web server for cancer and normal gene expression profiling and interactive analyses. *Nucleic Acids Res.* 45, W98–W102. doi: 10.1093/nar/gkx247
- Ultanir, S. K., Yadav, S., Hertz, N. T., Oses-Prieto, J. A., Claxton, S., Burlingame, A. L., et al. (2014). MST3 kinase phosphorylates TAO1/2 to enable Myosin Va function in promoting spine synapse development. *Neuron* 84, 968–982. doi: 10.1016/j.neuron.2014.10.025
- Xie, C., Mao, X., Huang, J., Ding, Y., Wu, J., Dong, S., et al. (2011). KOBAS 2.0: a web server for annotation and identification of enriched pathways and diseases. *Nucleic Acids Res.* 39, W316–W322. doi: 10.1093/nar/gkr483
- Xie, L., Wang, Q., Dang, Y., Ge, L., Sun, X., Li, N., et al. (2019). OSkirc: a web tool for identifying prognostic biomarkers in kidney renal clear cell carcinoma. *Future Oncol.* 15, 3103–3110. doi: 10.2217/fon-2019-0296
- Yu, F. X., Zhao, B., and Guan, K. L. (2015). Hippo pathway in organ size control. Tissue Homeostasis, and Cancer. *Cell* 163, 811–828.
- Zou, Q., Jin, J., Xiao, Y., Hu, H., Zhou, X., Jie, Z., et al. (2015). T cell development involves TRAF3IP3-mediated ERK signaling in the Golgi. *J. Exp. Med.* 212, 1323–1336. doi: 10.1084/jem.20150110

Conflict of Interest: The authors declare that the research was conducted in the absence of any commercial or financial relationships that could be construed as a potential conflict of interest.

Copyright © 2020 Xie, Wen and Qin. This is an open-access article distributed under the terms of the Creative Commons Attribution License (CC BY). The use, distribution or reproduction in other forums is permitted, provided the original author(s) and the copyright owner(s) are credited and that the original publication in this journal is cited, in accordance with accepted academic practice. No use, distribution or reproduction is permitted which does not comply with these terms.